ELSEVIER

Journal of Nuclear Materials 313–316 (2003) 1161–1166

journal of nuclear materials

www.elsevier.com/locate/jnucmat

Transport analysis of tungsten impurity in ITER

Y. Murakami [a,*], T. Amano [b], K. Shimizu [c], M. Shimada [d]

[a] Power & Industrial Systems R&D Center, Toshiba Corp., 4-1, Ukishima-cho, Kawasaki-ku, 210-0862 Kawasaki, Japan
[b] National Institute for Fusion Science, Toki, Gifu 509-5292, Japan
[c] Naka Fusion Research Establishment, JAERI, Naka-machi, Ibaraki 311-0193, Japan
[d] ITER International Team, Naka-machi, Naka-gun, Ibaraki 311-0193, Japan

Abstract

The radial distribution of tungsten impurity in ITER is calculated by using the 1.5D transport code TOTAL coupled with NCLASS, which can solve the neo-classical impurity flux considering arbitrary aspect ratio and collisionality. An impurity screening effect is observed when the density profile is flat and the line radiation power is smaller than in the case without impurity transport by a factor of 2. It is shown that 90 MW of line radiation power is possible without significant degradation of plasma performance ($H_{H98(y,2)} \sim 1$) when the fusion power is 700 MW (fusion gain $Q = 10$). The allowable tungsten density is about $7 \times 10^{15}/m^3$, which is 0.01% of the electron density and the increase of the effective ionic charge Z_{eff} is about 0.39. In this case, the total radiation power is more than half of the total heating power 210 MW, and power to the divertor region is less than 100 MW. This operation regime gives an opportunity for high fusion power operation in ITER with acceptable divertor conditions. Simulations for the case with an internal transport barrier (ITB) are also performed and it is found that impurity shielding by an ITB is possible with density profile control.

PACS: 52.25.Fi
Keywords: Transport; ITER; Impurity; Tungsten; NCLASS

1. Introduction

Most present fusion devices adopt low-Z (atomic number) materials such as carbon or beryllium as plasma-facing components. In a fusion reactor, however, the use of high-Z material such as tungsten is considered because of its low erosion rate. ITER also uses tungsten for the divertor baffles suggesting the possibility of introducing tungsten into the core plasma. Although the line radiation from high-Z materials has unfavorable influences in general, it has a beneficial effect of effectively reducing the divertor heat load. High heat load on the target plates in a fusion reactor is still a matter of concern and a possible solution is impurity seeding into the scrape-off layer (SOL) region and/or core plasma. Tungsten impurities which enter the core plasma can be used for this purpose, at least in principle, if excess accumulation can be avoided.

According to neo-classical theory [1], a finite gradient of plasma temperature has the effect of impurity shielding if the electron density gradient is small. While the density gradient of ITER is very small in the reference operation point [2], operation with a peaked density profile is also planned for an advanced operation mode with an internal transport barrier (ITB). In many experiments [3,4], the inward pinch of impurity particles is observed in the presence of an ITB. Therefore, the behavior of tungsten impurity in the ITER plasma is an important issue.

The present work investigates impurity behavior in the core plasma under the assumption that impurity fluxes are dominated by neo-classical transport [5]. Therefore, this work may serve as a reference of the worst case with respect to impurity accumulation. The

* Corresponding author. Tel.: +81-44 288 8122; fax: +81-44 270 1806.
E-mail address: yoshiki.murakami@toshiba.co.jp (Y. Murakami).

0022-3115/03/$ - see front matter
PII: S0022-3115(02)01512-X

radial distribution of tungsten impurity in ITER is calculated for various density profiles by using a 1.5D transport code. The impurity transport in the SOL and divertor region is not solved here and the transport in the core plasma is calculated by assuming the tungsten flux at the separatrix. In Section 2, simulation codes used in this paper are described. In Section 3, a density profile survey is made. In Section 4, the line radiation power is estimated. In Section 5, simulation results for plasmas with an ITB are presented. Section 6 is the summary.

2. Code description

Simulations are carried out with the 1.5D transport code TOTAL [6]. The transport equations solved in the TOTAL code are similar to those in the PRETOR code [7]. For the anomalous part of the transport coefficients, a Bohm-type model [8] is used.

$$\chi_e = \chi_i = \alpha_B \frac{T_e}{B_T} q_\Psi^2 / L_{Pe}^*, \tag{1}$$

where T_e, B_T and q_Ψ are the electron temperature, toroidal magnetic field and MHD safety factor, respectively. L_{pe}^* is the scale length of the pressure gradient normalized by the minor radius and α_B is determined to achieve the given fusion power at the reference operation point. The particle diffusion coefficient $D_{i,e}$ is assumed to be $\chi_{i,e}/4$. The calculation of impurity flux is done by the NCLASS code [9], which can include arbitrary aspect ratio and collisionality. Here, the neoclassical impurity flux Γ_k^{neoc} is expressed by

$$\Gamma_k^{neoc} = -D_k^{neoc}\nabla n_k + D_k^{neoc} n_k \left[\sum_{l \neq k} \left(g_{n_{l\to k}} \frac{\nabla n_l}{n_l} \right) + g_{T_i} \frac{\nabla T_i}{T_i} + g_{T_e} \frac{\nabla T_e}{T_e} \right], \tag{2}$$

where n_k and D_k^{neoc} are the density and the particle diffusion coefficient of the kth ionic charge state of the impurity. g_{n_i}, g_{T_i} and g_{T_e} denote the screening/pinch effects of the density gradient, ion temperature gradient and electron temperature gradient, respectively. Typically, the density gradient terms cause the impurity pinch effect and the temperature gradient terms lead to a screening effect. In this code, collisions between the different impurity species are also included.

The density n_k of impurity ions of a charge state k is obtained by solving the rate equation;

$$\frac{\partial n_k}{\partial t} = -\frac{\partial}{V'\partial\rho}\left[V'\Gamma_k\right] - (S_{k+1} + \alpha_{k-1})n_k + S_k n_{k-1} + \alpha_k n_{k+1}, \tag{3}$$

where V denotes the volume element given by a 2D equilibrium calculation, ρ is the radial co-ordinate label of the magnetic surface, $V' = dV/d\rho$, and, S_k and α_k denote the ionization coefficient and recombination coefficient, respectively. Here, cooling rates by electron-impact excitation, ionization, bremsstrahlung, radiative recombination and di-electronic recombination are included, but ion-impact excitation is not included. Cooling rates are calculated by the ADPAK code [10] and rate coefficients are modified using the results of Fournier [11].

The boundary conditions are given by the characteristic length of the impurity density at the plasma edge. That is,

$$-\frac{1}{n_k}\frac{dn_k}{d\rho}\bigg|_{\rho=1} = \frac{1}{\Delta}. \tag{4}$$

In the present paper, it is assumed that $\Delta = 2.5$ cm. At the plasma edge, the incoming neutral flux is balanced by an outward impurity flux

$$\Gamma_0 = \sum_k \left[-\left(D_k^{ano} + D_k^{noec}\right)\frac{\partial n_k}{\partial\rho} + n_k v_k \right]. \tag{5}$$

Here, D_k^{ano} is the anomalous part of diffusion coefficient and v_k is the radial velocity coming from the terms for ∇n and ∇T. The neutral tungsten density profile is given by

$$v_0 \frac{\partial n_0}{\partial\rho} = S_0 n_e n_0. \tag{6}$$

Here, v_0 is the neutral tungsten velocity and S_0 is the ionization coefficient (assuming 10 eV). The electron density, electron temperature and ion temperature are given at the plasma surface as boundary conditions.

3. Density profile survey

The simulations are carried out with the parameters of ITER (major radius 6.2 m, minor radius 2 m, plasma elongation 1.7, triangularity 0.35, center toroidal field 5.3 T and plasma current 15 MA).

Fig. 1 shows tungsten profiles for various electron density profiles. Here, the density profile is changed by controlling the gas-puff rate for a given separatrix density $n_{e,S}$ when the fusion power is kept at 400 MW. Plasma edge temperatures (T_e, T_i) are fixed to 1 keV. The tungsten flux at the plasma surface is adjusted so that the tungsten density at the separatrix has a given value $n_{W,S} = 0.2 \times 10^{15}/m^3$. When the electron density profile is not flat (solid line), the impurity velocity (V_{imp}) is negative (inward) in the peripheral region and an increase of the tungsten density (n_W) is observed. When the density profile is relatively flat, the impurity velocity

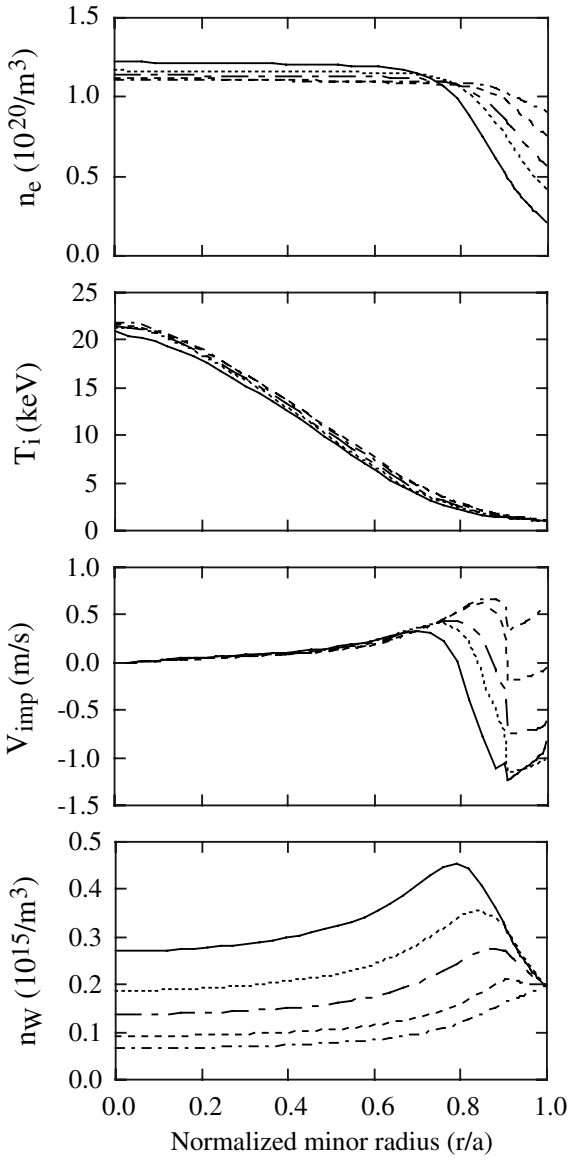

Fig. 1. Tungsten density profiles (n_W) for various electron density profiles (n_e) with separatrix density $n_{e,S} = 0.2 \sim 0.9 \times 10^{20}$/m^3. Here, the fusion power is fixed to 400 MW and the tungsten flux at the plasma surface is adjusted so that $n_W(1) = 0.2 \times 10^{15}$/m^3.

is positive (outward) over most of the plasma radius and over this region the tungsten density increases monotonically with minor radius (impurity shielding effect).

4. Achievable line radiation power in ITER

Operation with larger fusion power (~700 MW, $Q = 10$) is also planned in ITER, when the total heating power is about 210 MW (alpha heating power $P_\alpha =$ 140 MW + additional heating power $P_{ADD} = 70$ MW). In this case, the divertor heat load could be too high. According to 2D divertor simulations with ITER geometry, power to the divertor targets can be reduced to the acceptable level when the power to the SOL is less than 100 MW [12]. Therefore, a half of the heating power should be radiated in the core plasma for the acceptable divertor operation as a rough estimation.

Fig. 2 shows the achievable line radiation power P_{LIN}^{TOT} and the corresponding HH-factor for various tungsten densities $n_{W,S}$ at the plasma edge. In this case, the electron density is increased with the tungsten density to maintain the fusion power at 700 MW. The increment in the electron density is, however, small (2–3%) even for the maximum tungsten density. The required HH-factor to achieve the fusion gain $Q = 10$ is calculated from the ITER98$(y, 2)$ scaling formula [13]. Here, open square symbols denote the case with a flat density profile and closed circles denote the case with a peaked density profile. It is seen that 90 MW of line radiation power is achieved in both cases. When the density profile is flat, a small improvement (~5%) of the HH-factor allows the addition of 7×10^{15}/m^3 of tungsten impurity, which is 0.01% of the electron density and the increase of the effective ionic charge Z_{eff} is about 0.39. In this case, the radiation power including bremsstrahlung and synchrotron radiation is more than half of the total heating power 210 MW and power to the divertor region is less than 100 MW. This value is small enough to satisfy the divertor condition [12]. Therefore, this operation regime gives an opportunity for high fusion power operation in ITER with acceptable divertor conditions. Open circles in Fig. 2 denote the case with the fixed impurity profile (same profile as electron density) calculated by the PRETOR code [7]. In this case, the acceptable tungsten density is 2–3 times smaller than that for the case with impurity transport (open squares), but the achievable line radiation is the same level as the previous case.

5. Simulation for plasma with ITB

If an ITB is formed, there exists a large density gradient in the plasma together with a temperature gradient. Therefore, the impurity shielding effect could be modified. Since the mechanism of ITB formation has not been clarified, the following simple transport model is assumed;

$$\chi_e = \chi_i = \chi_0(1 + \rho^2)E(s),$$
$$E(s) = \{1 + \exp[c(s+1)]\}^{-1} + \{1 + \exp[-c(s-1)]\}. \quad (7)$$

Here, s is a shear parameter and c is adjusted so that the transport coefficient is reduced to 1/10 at $s = 0$ ($E(s) \sim 1$

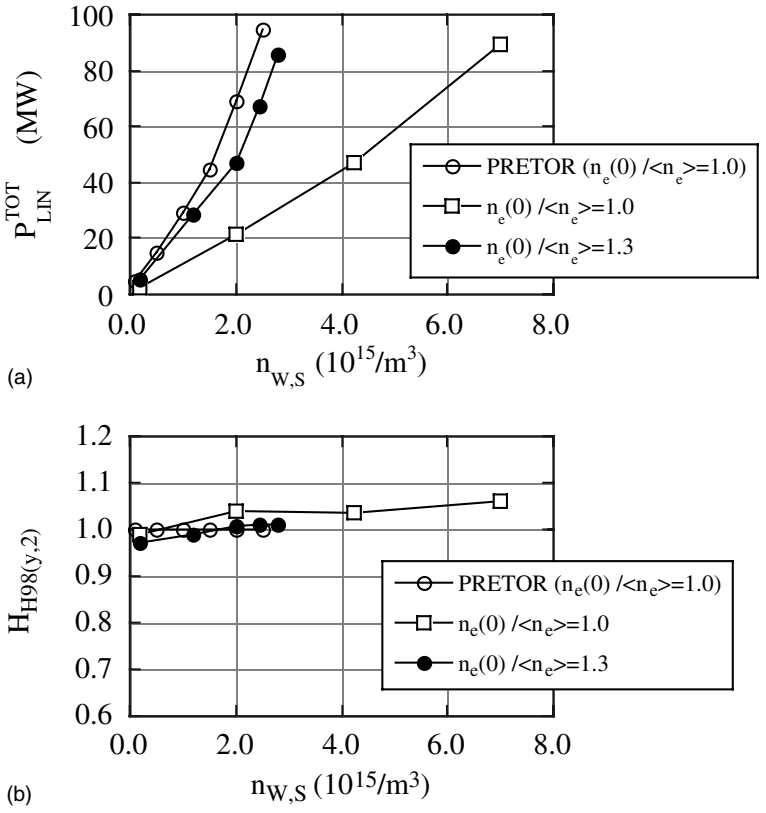

Fig. 2. (a) Relation between tungsten density $n_{W,S}$ at the plasma edge and the total line radiation power P^{TOT}_{LIN}. (b) Required HH-factor to achieve $Q = 10$ and 700 MW calculated from ITER98$(y, 2)$ scaling.

almost everywhere and takes a minimum value at $s = 0$). In this paper, s is replaced by $20(r - r_{ITB})/a$ to create an ITB artificially. χ_0 is determined to achieve a given HH-factor ($\sim$1.0). This model is used to obtain typical density and temperature profiles in the ITB plasma. In this section, the standard operation case (fusion power = 400 MW, $Q = 10$) is considered.

Fig. 3 shows the time development of plasma parameters when the ITB is formed. Here, P_α, P_{ADD}, P_{RAD}, P_{SYN} and P_{LIN} are alpha heating power, additional heating power, total radiation power including bremsstrahlung radiation, synchrotron radiation power and line radiation power, respectively. In the simulation, a step-like increase of neutral tungsten flux ($\Gamma_{W,S} = 5 \times 10^{18}$/s) at the plasma surface is given at $t = 200$ s and an ITB is formed at $t = 250$ s. It is seen that the line radiation power decreases when the ITB is formed.

Fig. 4 shows plasma parameter profiles at $t = 300$ s in Fig. 3. The ITB is formed around $r/a \sim 0.75$, where the transport coefficient is decreased artificially. The impurity velocity profile (V_{imp}) and tungsten fraction profile ($f_W = n_W/n_e$) are also shown in Fig. 4. It is seen that the

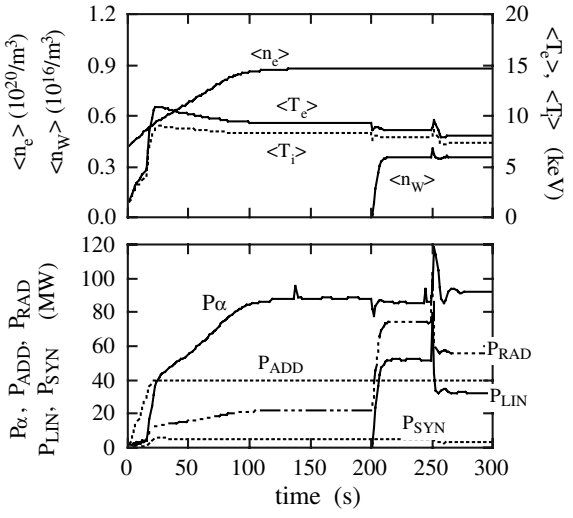

Fig. 3. Time development of plasma parameters when an ITB exists. Here, fusion power is 400 MW, tungsten impurity is injected at $t = 200$ s ($\Gamma_{W,S} = 5 \times 10^{18}$/s) and an ITB is formed at $t = 250$ s.

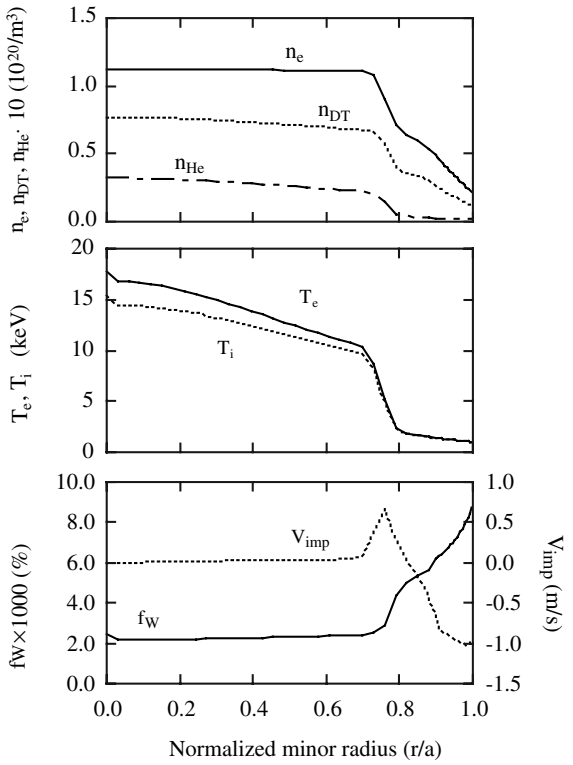

Fig. 4. Plasma parameter profiles after the ITB is formed ($t = 300$ s) in Fig. 3. Here, $f_W = n_W/n_e$, and V_{imp} is the radial velocity of tungsten ions.

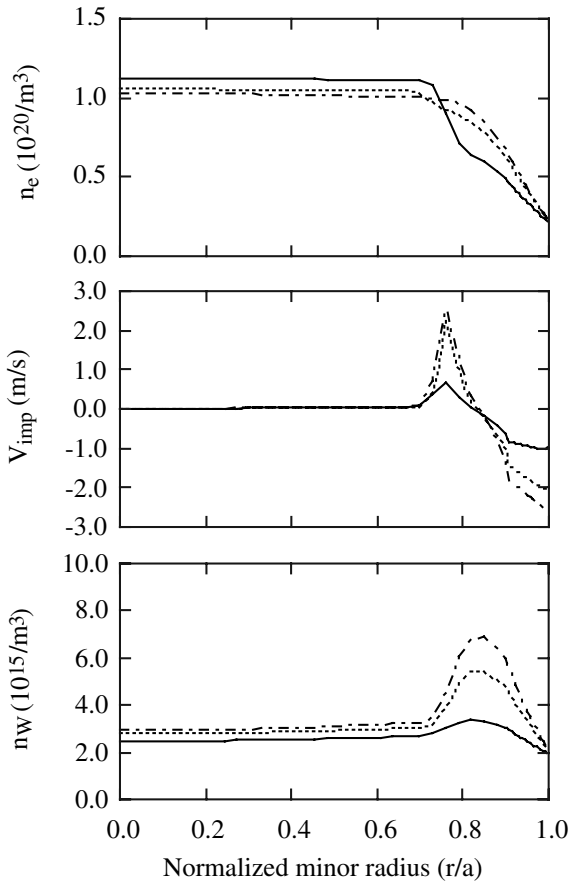

Fig. 5. Plasma parameter profiles for various ITB shapes. Here, n_W and V_{imp} is the density and the radial velocity of tungsten ions. Solid line, dotted line and short-long dashed line correspond to the different density profiles. Temperature profile is the same as that of Fig. 4.

impurity velocity is positive around the ITB, which implies the impurity shielding effect. In this case, the outward impurity velocity is increased when the ITB is formed. In the present model, the shielding effect on impurities as a result of the temperature gradient dominates the density gradient effect. When the radial position of the foot point of the density gradient is different from that of the temperature gradient as in the Ref. [3], the shielding is not effective and impurity accumulation is observed (see Fig. 5). These results imply that impurity shielding is possible even in an ITB plasma by controlling the density profile.

6. Summary

The impurity behavior in the core plasma of ITER is investigated by a multi-species fluid model. The 1.5D transport code TOTAL coupled with the NCLASS code is used. An impurity screening effect due to temperature gradients is observed when the density profile is flat. It is shown that 90 MW of line radiation power is possible without significant degradation of plasma performance ($H_{H98(y,2)} \sim 1$) when the fusion power is 700 MW ($Q = 10$). When the density profile is flat, a small improvement (~5%) of the HH-factor allows the addition of $7 \times 10^{15}/m^3$ of tungsten impurity, which is 0.01% of electron density and the increase of effective ionic charge Z_{eff} is about 0.39. In this case, the radiation power including bremsstrahlung and synchrotron radiation is more than half of the total heating power 210 MW, and power to the divertor region is less than 100 MW. This operation regime makes possible high fusion power operation in ITER with consistent divertor conditions. Refinement of atomic data including the fast ion effect [14] is necessary to improve the precision of the permissible level of the impurity. Simulation of an ITB plasma shows the possibility of impurity shielding by density profile control. Since there is a wide variety of plasma profiles for this type of operation mode, further work is necessary. Comparison between simulation results and experimental observation is also an important future work.

Acknowledgements

The authors wish to thank Drs Y. Shimomura, M. Sugihara and other members of ITER International Team for useful discussions. The authors also would like to thank Drs T. Shoji, T. Tsunematsu and K. Ushigusa, and Professor Y. Ogawa for their continued encouragement. One of the authors (Y.M) expresses his gratitude to Drs Y. Uenohara, M. Kawashima and M. Kondo of Toshiba Corp., for providing the opportunity to work in the ITER-JCT.

References

[1] S.P. Hirshman, Phys. Fluids 20 (1977) 589.
[2] Y. Murakami et al., J. Plasma Fusion Res. 77 (2001) 712.
[3] R. Dux et al., 28th EPS Conference, Funchal, 2001, p. 505.
[4] H. Takenaga et al., J. Plasma Fusion Res. 75 (1999) 952.
[5] R. Dux, A.G. Peeters, Nucl. Fusion 40 (2000) 1721.
[6] T. Amano et al., IPPJ-616, 1982.
[7] D. Boucher et al., in: Proc. 16th IAEA Fusion Energy Conference, Montréal, 1996, IAEA, Vienna, 1997, p. 945.
[8] A. Taroni et al., Plasma Phys. Control. Fusion 36 (1994) 1629.
[9] W.A. Houlberg et al., Phys. Plasmas 4 (1997) 3230.
[10] D.E. Post et al., At. Data Nucl. Data Tables 20 (1977) 397.
[11] K.B. Fournier, At. Data Nucl. Data Tables 68 (1998) 1.
[12] A. Kukushkin et al., 18th Fusion Energy Conference, Sorrento, 2000, IAEA-CN-77/ITER/2.
[13] ITER Physics Basis, Nucl. Fusion 39 (1999) 2137.
[14] V.A. Abramov, A.R. Polevoi, in: Proc. 16th IAEA Fusion Energy Conference, Montréal, 1996, IAEA, Vienna, 1997, p. 619.